Experimental Study on Edge Confinement of Reinforced Concrete Core Walls

R. Tokunaga
DKshiken Co., Ltd., Japan

T. Nakachi
Fukui University of Technology, Japan

SUMMARY:
In the core wall system in high-rise buildings, the four L-shaped core walls at the center are subjected to high axial load under diagonal seismic force. In particular, the corner and the area near the corner of an L-shaped core wall are exposed to high compressive stress, and should be reinforced to improve the deformation capacity of the core walls. In this study, lateral loading tests were conducted on eleven wall columns simulating the corner and the area near the corner of L-shaped core walls. The test parameters were the number of confining bars, type of concrete confinement, level of axial stress and presence/absence of the hook. Based on the results of the lateral loading tests, the effect of edge confinement on the deformation capacity of core walls was clarified.

Keywords: Reinforced concrete, core wall, deformation capacity, confining steel, hook

1. INTRODUCTION

Reinforcing the areas of core walls that come under high compressive stress is considered effective for improving their deformation capacity. Previously, we conducted lateral loading tests on multistory L-shaped reinforced concrete core walls and examined the relationship between the confinement effect of these areas and the deformation capacity of the core walls.[1] We also conducted central compression tests and eccentric compression tests on square and rectangular section columns simulating the corner and the area near the corner of L-shaped core walls.[2] In the present study, lateral loading tests were conducted on eleven wall columns simulating the area near the corner of L-shaped core walls in order to examine the effect of the edge confinement on the deformation capacity of core walls.

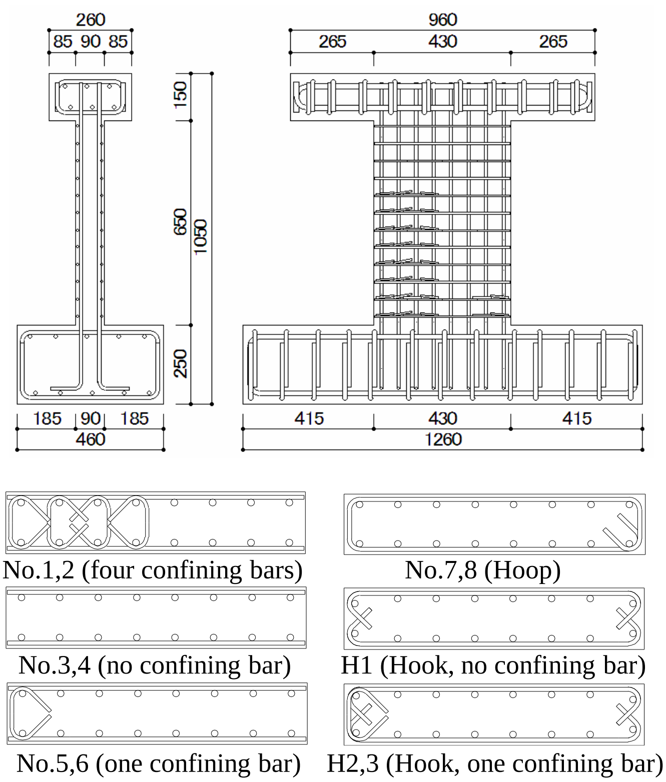

Fig. 1 Test Specimens

2. SUMMARY OF TESTS

2.1 Test Specimens

The configuration and arrangement of reinforcement provided in the specimens are shown in Fig. 1.

The characteristics of the specimens are listed in Table 1. The physical properties of the concrete and reinforcement are listed in Table 2 and Table 3, respectively. Eleven one-eighth-scale wall column specimens simulating the area near the corner of L-shaped core walls were tested. Each specimen represented the lower three stories of a high-rise building of approximately twenty-five stories. The specimens had rectangular cross sections measuring 90×430 mm, were the flexural type and had a shear span ratio of 2. 79. The specified design strength of the concrete (Fc) was 60 N/mm^2 and the ratio of axial stress to concrete compressive cylinder strength (axial stress ratio) was 0.2 in Specimens 1, 3, 5, 7 and H3. The specified design strength of the concrete was 33 N/mm^2 and the axial stress ratio was 0.4 in Specimens 2, 4, 6, 8, H1 and H2. D10 and D6 deformation bars with yield strength of 393 and 372 N/mm^2 were used for longitudinal and transverse reinforcement, respectively. High-strength bar U5.1 with yield strength of 1368 N/mm^2 was used for the confining bars.

Table 1 Characteristics of Specimens

Specimen	Fc (N/mm^2)	Axial Stress Ratio	Axial Load (kN)	Number of Confining Bars
No.1	60	0.2	489	4
No.2	33	0.4	495	
No.3	60	0.2	474	0
No.4	33	0.4	503	
No.5	60	0.2	500	1
No.6	33	0.4	534	
No.7	60	0.2	461	0(Hoop)
No.8	33	0.4	539	
H1	33	0.4	553	0(Hook)
H2	33	0.4	534	1(Hook)
H3	60	0.2	461	

Table 2 Physical Properties of Concrete

Specimen	Compressive Strength (N/mm^2)	Young's Modulus (×10^{4}N/mm^2)	Sprit Strength (N/mm^2)
No.1	63.2	2.90	3.40
No.2	32.0	2.25	1.69
No.3	61.3	2.71	2.62
No.4	32.5	2.00	2.52
No.5	64.6	2.83	3.17
No.6	34.5	2.03	1.81
No.7	59.6	2.89	2.46
No.8	34.8	2.09	2.60
H1	35.7	2.13	1.74
H2	34.8	2.15	1.82
H3	60.9	3.01	3.66

The test parameters were the number of confining bars, type of concrete confinement, level of axial stress and presence/absence of the hook. Tie bars were used for the confining bars and the number of confining bars varied according to the horizontal number of tie bars. The type of concrete confinement was tie bars and hoops. The axial stress ratio was 0.2 and 0.4. Both ends of transverse reinforcement were anchored in the specimens with hooks. The confining bars were arranged up to a height corresponding to the width of the wall column (h: 430 mm). Specimen cover concrete was 5 mm thick.

Table 3 Physical Properties of Steel

Bar Size	Yield Strength (N/mm^2)	Maximum Strength (N/mm^2)	Young's Modulus (×10^{5}N/mm^2)	Elogation (%)
D10	393	568	2.04	25.8
D6	372	524	2.05	25.7
U5.1	1368	1491	2.11	9.3

The specimens were designed so that the shear strength would be larger than the flexural strength. Specimens 1 and 2 had four confining bars in the cross section, Specimens 5, 6, H2 and H3 had one confining bar, and Specimens 3, 4 and H1 had no confining bar. Specimens 7 and 8 had the hoop. Specimens H1, H2 and H3 had hooks at both ends of transverse reinforcement.

2.2 Test Procedure

The loading test was the cantilever type, as shown in Fig. 2. In the cyclic lateral loading test, the specimen was subjected to lateral forces by a horizontal hydraulic jack connected to the reaction frame. Constant axial loading force was applied by a vertical hydraulic jack over the specimen to represent the axial stress in the stage of coupling beam yielding at the center core. The axial stress ratio was 0.2 or 0.4 under positive loading for which the corner area of L-shaped core walls is compressive and 30 kN under negative loading, respectively. Loading was controlled by the horizontal drift angle at a

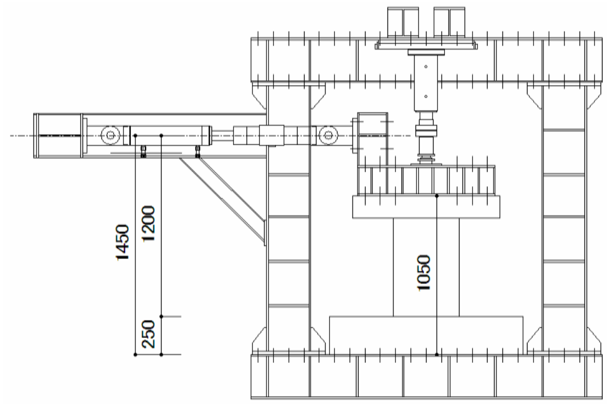

Fig. 2 Loading System

height corresponding to the second floor level (h: 615mm). The loading was cyclic lateral loading at R (drift angle) = 1/1000 (rad.) (1 cycle), 2/1000, 5/1000, 7.5/1000, 10/1000, 15/1000, 20/1000 (2 cycle respectively), 30/1000, 40/1000 (1 cycle respectively). Relative displacement was measured by displacement transducers, such as the expansion and contraction of each segment. Strain gages were attached to the confining bar, the longitudinal reinforcement and the transverse reinforcement. The attachment position of strain gages at the confining bar was the midpoint of the tie bar.

3. TEST RESULTS

3.1 Fracture Process

The crack patterns of specimens during the final stage are shown in Fig. 3. Under negative loading, flexural cracks occurred at the bottom of all specimens. After that, flexural cracks expanded upward and to the middle of the specimens. Under positive loading of all specimens, the longitudinal reinforcement at the compressive end yielded (yield strain 1926×10^{-6}) at approximately 5/1000, and the longitudinal reinforcement at the tensile end yielded under negative loading. Under both positive and negative loading, flexural shear cracks occurred at approximately 7.5/1000. The corner area at the bottom appeared to crack vertically and crumbled slightly at 5/1000 to 7.5/1000. At the final stage, all the specimens crumbled, buckling of the longitudinal reinforcement was observed, and the strength decreased under positive loading.

3.2 Load Deflection Curves

The maximum strength and the limit drift angle are listed in Table 4. Figure 4 shows the load deflection

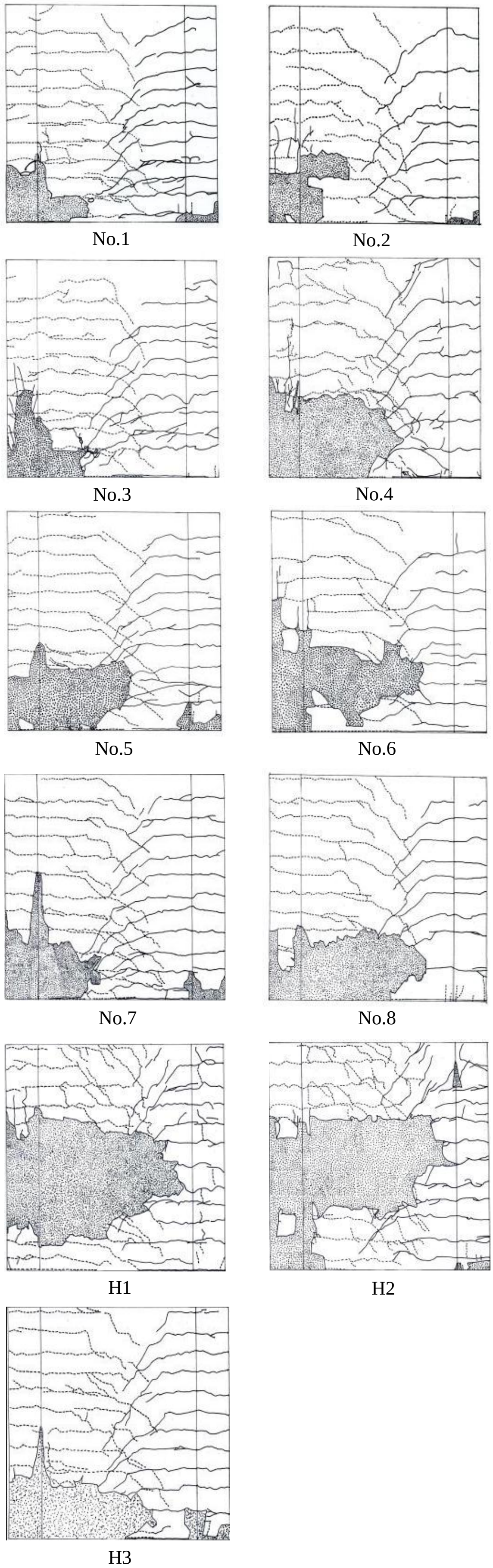

Fig. 3 Crack Patterns

Table 4 Test Results

Specimen	Maximum Strength			Limit Drift Angle (×1/1000rad.)	Limit Drift Angle Ratio
	Exp. Load (kN)	Cal. Load (kN)	Exp/Cal		
No.1	107.3	102.0	1.05	30.0	1.49
No.2	94.2	84.1	1.12	25.5	1.45
No.3	114.1	98.7	1.16	20.1	1.00
No.4	100.1	84.8	1.18	17.6	1.00
No.5	126.1	102.4	1.23	24.5	1.22
No.6	102.9	88.1	1.17	19.2	1.09
No.7	119.9	96.8	1.24	28.8	1.44
No.8	109.2	88.6	1.23	24.2	1.38
H1	111.5	90.1	1.24	16.6	0.95
H2	111.7	88.4	1.26	28.4	1.62
H3	120.0	97.2	1.23	30.2	1.50

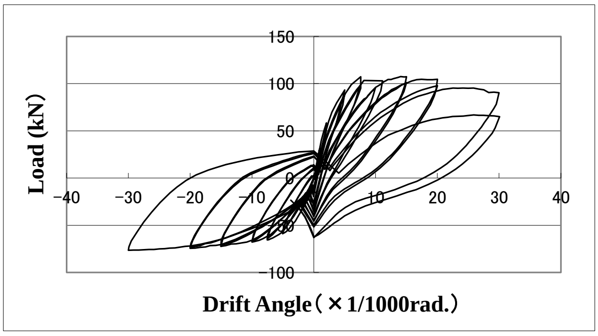

No.1

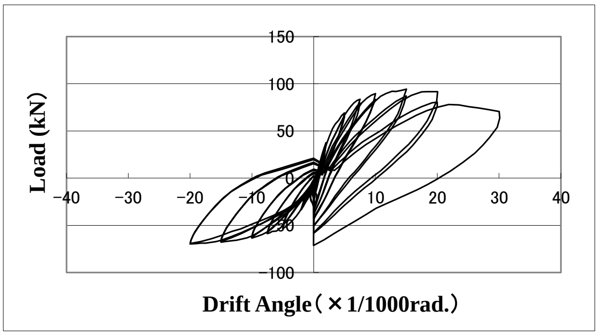

No.2

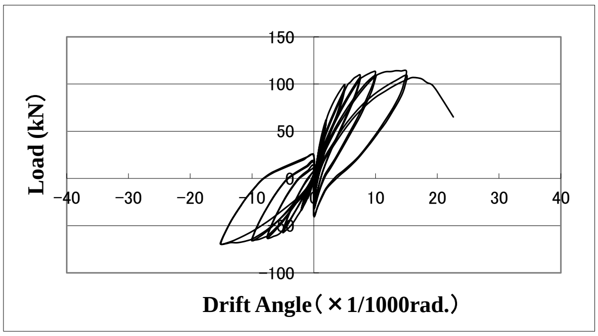

No.3

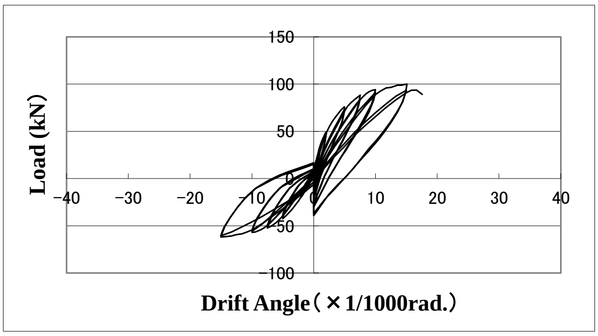

No.4

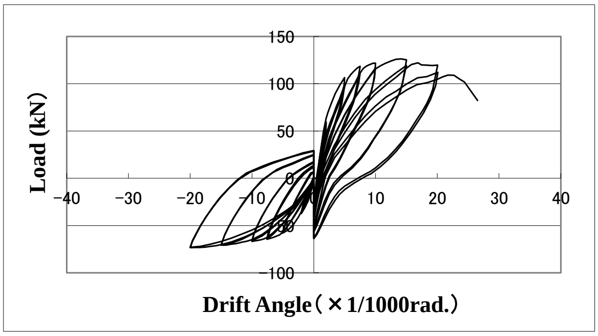

No.5

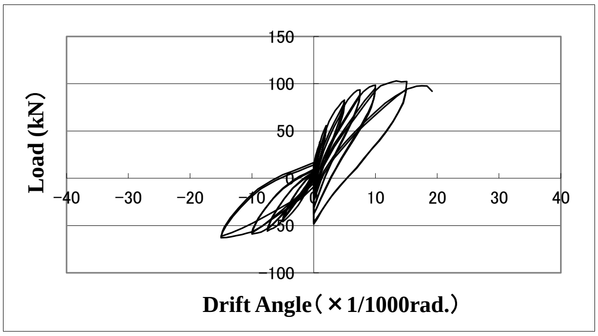

No.6

Fig. 4(a) Load - Deflection Curve

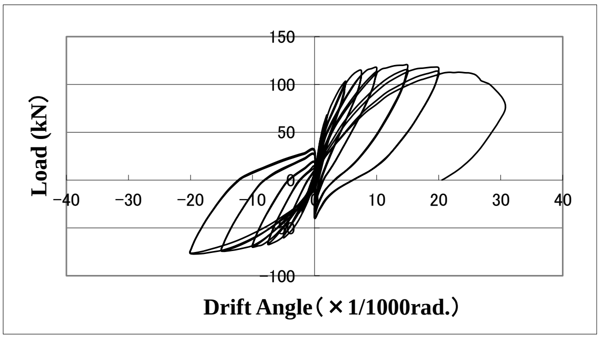

No.7

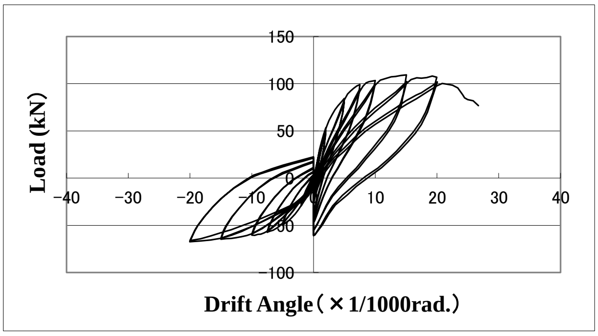

No.8

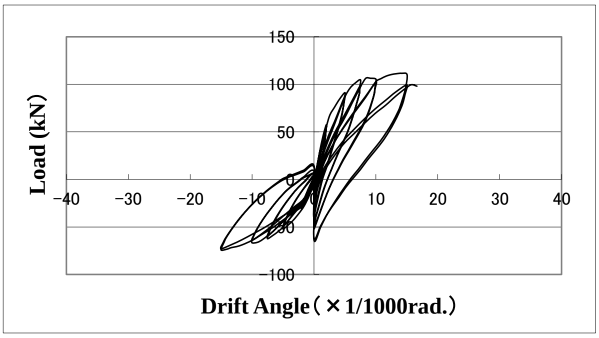

H1

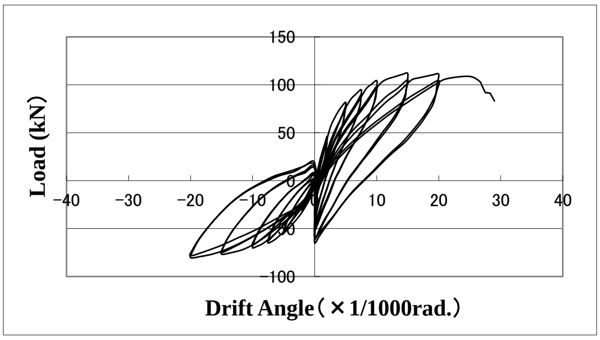

H2

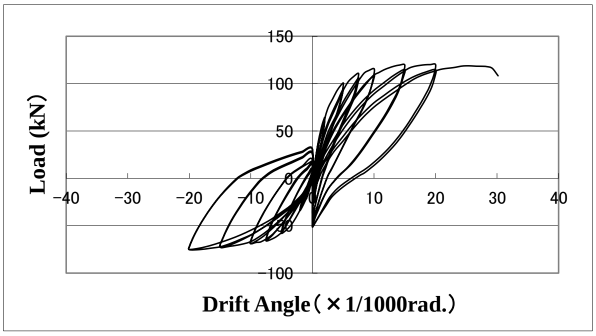

H3

Fig. 4(b) Load **-** Deflection Curve

curves. Regarding the maximum strength, all experimental results were larger than that calculated by the equation previously mentioned (AIJ 1990). [3)] In the figure, the load deflection loops are discontinuous as the axial load changed at R = 0. The relationship between the load and the deflection during the final stage was as follows. The load of Specimen 1 decreased largely during the cycle of 40/1000 and the loading test finished at 30/1000. The load of Specimen 2 decreased largely during the cycle of 30/1000. Specimen 3, which had a rapid decrease in load, could not withstand the axial load the moment the drift angle reached 20/1000 during the first cycle of 20/1000. Specimens 4, 6 and H1, which had a rapid decrease in load, could not withstand the axial load during the first cycle of 20/1000. Specimens 5, 8 and H2 had a rapid decrease in load and could not withstand the axial load during the cycle of 30/1000. The load of Specimen 7 decreased largely during the cycle of 30/1000 and the loading test finished at 30/1000. Specimen H3 had a rapid decrease in load and could not withstand the axial load the moment the drift angle reached 30/1000 during the cycle of 30/1000.

Specimens 1 and 2 with four confining bars withstood the axial load during the cycle of 30/1000. On the other hand, the other specimens except for Specimen 7 with an axial stress ratio of 0.2 could not withstand the axial load and the horizontal load decreased rapidly at the final stage. Therefore, it is considered that the specimens can withstand the axial load up to 30/1000 by arranging the confining bars further inside the cross section.

Comparison of the specimens at the final stage by the axial stress ratio revealed the following. The limit drift angle of Specimen 2 with an axial stress ratio of 0.4 was during the first cycle of 30/1000. On the other hand, the load of Specimen 1 with an axial stress ratio of 0.2 was more than 80% of the maximum strength during the first cycle of 30/1000. In the case of Specimens 3 and 4 without the confining bars and Specimens 5 and 6 with a confining bar, Specimens 3 and 5 with an axial stress ratio of 0.2 were not able to withstand the axial load after the load decreased to some extent. On the other hand, Specimens 4 and 6 with an axial stress ratio of 0.4 were not able to withstand the axial load without decrement of the load. Therefore, specimens with a higher axial stress ratio are considered to fracture more rapidly.

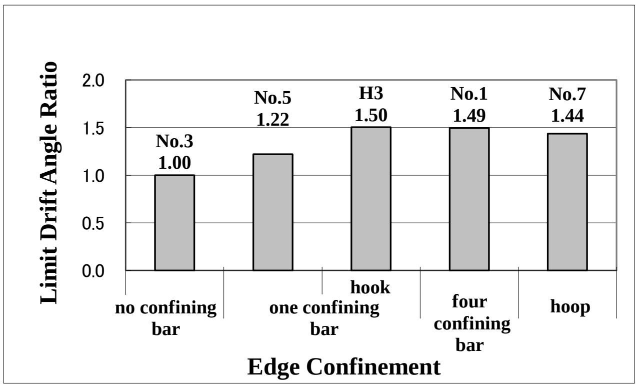

Fig. 5(a) Comparison of Limit Drift Angle Ratio (Axial Stress Ratio of 0.2)

The effect of the hoop on decrement of the load at the final stage was as follows. In the case of specimens with an axial stress ratio of 0.2, Specimen 3 without the confining bar and Specimen 5 with a confining bar had a rapid decrease in load at the final stage and could not withstand the axial load. On the other hand, Specimen 7 with the hoop had a gradual decrease in load at the final stage and withstood the axial load until the completion of lateral loading. In the case of specimens with an axial stress ratio of 0.4, Specimen 4 without the confining bar and Specimen 6 with a confining bar had a rapid decrease in load at the final stage and could not withstand the axial load. On the other hand, Specimen 8 with the hoop had a slight decrease in load, and after that, had a rapid decrease and was not able to withstand the axial load. Therefore, the hoop is considered to be effective for the gradual decrement of the lateral load at the final stage.

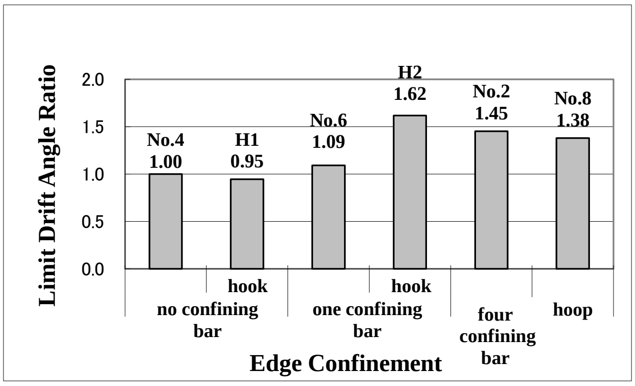

Fig. 5(b) Comparison of Limit Drift Angle Ratio (Axial Stress Ratio of 0.4)

3.3 Relationship between Edge Confinement and Deformation Capacity

The limit drift angles are listed in Table 4. Figure 5 shows a comparison of the limit drift angle ratio. The limit drift angle is defined as the maximum drift angle at which the specimen retains 80% of the maximum strength. The limit drift angle ratio is the ratio of the limit drift angle of each specimen to that of Specimens 3 and 4 without the confining bars at an axial stress ratio of 0.2 and 0.4, respectively.

The limit drift angle ratios of Specimen 1 with four confining bars and Specimen 5 with one confining bar were 1.49 and 1.22, respectively, at an axial stress ratio of 0.2. Similarly, that of Specimens 2 and 6 were 1.45 and 1.09, respectively, at an axial stress ratio of 0.4. That is, the larger drift angle ratio of a specimen corresponded to the larger number of confining bars. It is considered that the compressive ductility of concrete at the edge area in Specimens 3 and 4 without the confining bar was small, and therefore the limit drift angles of these specimens were smaller than that of other specimens confined at the edge area. It is also considered that the compressive ductility of concrete at the edge and inside area of Specimens 1 and 2 with four confining bars was large, and therefore the limit drift angles of these specimens were larger than that of Specimens 5 and 6 with one confining bar. The compressive ductility at the edge area in Specimens 7 and 8 is considered to have increased with the confinement effect of concrete due to the presence of the hoop.

In comparing the same arrangement of specimens with different axial stress ratios, the drift angles of Specimens 2, 4, 6 and 8 with an axial stress ratio of 0.4 were smaller than that of Specimens 1, 3, 5 and 7 with an axial stress ratio of 0.2, respectively. That is, the drift angle is smaller for specimens with a larger axial stress ratio. The reason for this is considered to be as follows. The vertical strain of the compressive edge at the bottom of the specimen with a large axial stress ratio is larger than that of the specimen with a small axial stress ratio at the same drift angle. Consequently, there is a decrease in the compressive stress that the specimen with a large axial stress ratio can withstand, and as a result, the concrete at the edge crumbles at an earlier stage.

In comparing the absence and presence of the hook, in the case of specimens without the confining bar, the drift angle ratio of Specimen H1 with the hook and that of Specimen 4 without the hook at an axial stress ratio of 0.4 were 0.95 and 1.0, respectively. That is, the drift angle ratios were approximately the same. On the other hand, in the case of specimens with the confining bar, at an axial stress ratio of 0.2, the drift angle ratio of Specimen H3 with the hook and that of Specimen 5 without the hook were 1.50 and 1.22, respectively. Similarly, at an axial stress ratio of 0.4, the drift angle ratio of Specimen H2 with the hook and that of Specimen 6 without the hook were 1.62 and 1.09, respectively. That is, in the case of specimens with the confining bar, the drift angle ratio of the specimen with the hook is larger than that of the specimen without the hook at both axial stress ratios of 0.2 and 0.4. The reason why the hook had no effect in the case of the specimen without a confining bar is considered to be as follows. Due to the lack of confining force in the thickness direction, the concrete at the compressive end crumbled before the confining force of the transverse reinforcement was increased by the hook.

3.4 Horizontal Strain Distribution of Confining Bar, Hoop and Transverse Reinforcement

Figure 6 shows the horizontal strain distribution of the confining bar and the hoop and the transverse reinforcement. Figures 6(a) and 6(b) show the strain distribution of the confining bar in Specimens 1 and 2 at a height of 82.5 mm, respectively. Figures 6(c) and 6(d) show the strain distribution of the hoop in Specimens 7 and 8 at a height of 82.5 mm, respectively. Figures 6(e), 6(f) and 6(g) show that of the confining bar and the transverse reinforcement in Specimens H1 and H2 at a height of 192.5 mm and Specimen H3 at a height of 137.5 mm, respectively. The strain was measured by strain gages attached to both sides of the confining bar or to the hoop at the neutral axis, and the strain values are the average of both sides. The attachment position of strain gages at the confining bar was the midpoint of the thickness direction of the specimen. The distribution was the longitudinal distribution in the cross section of the specimen, and at the peak of positive loading at each drift angle. The figures show the relationship between the strain of the confining bar or hoop and the distance from the compressive end.

The strain of the confining bars in Specimens 1 and 2 with four confining bars increased with the increment in drift angle at all measuring points up to 20/1000. The strain was larger at points nearer to the compressive end. The reason for this tendency is considered to be that the compressive stress and strain of concrete was larger at the area nearer to the compressive end and therefore the confining force by the confining bar increased. The strain of the confining bars in Specimen 1 was small at a point 130 mm from the compressive end and was almost 0 at a point 190 mm away. That is, the area from the compressive end to a point approximately 130 mm from the compressive end was considered to be the high compressive area. On the other hand, in Specimen 2 with increased axial stress ratio, the strain occurred at points 130 mm and 190 mm from the end after 20/1000. That is, the area up to a point approximately 190 mm from the end was considered to be the high compressive area. The reason for this result is considered to be that the high compressive area was extended by the increment in the axial stress ratio.

The strain of the hoop in Specimens 7 and 8 also increased with the increment in drift angle at all measuring points. The strain was larger at the points nearer to the compressive end. The increment of strain near the compressive end in Specimen 7 with an axial stress ratio of 0.2 was remarkable compared with that in Specimen 8 with an axial stress ratio of 0.4. Particularly, the strain at a point 22.5 mm from the compressive end at the final stage was very large at approximately 4500×10^{-6}. The reason for this large strain is considered to be that the neutral axis depth of Specimen 7 with an axial stress ratio of 0.2 was smaller than that of Specimen 8 with a ratio of 0.4 and therefore the strain was concentrated at the compressive end. On the other hand, the increment of strain at the compressive end

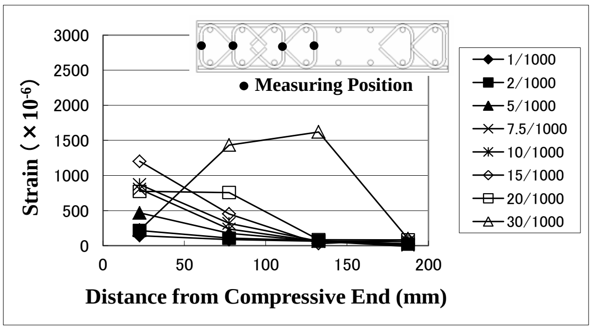

Fig. 6(a) Horizontal Strain Distribution of Confining bars (No.1)

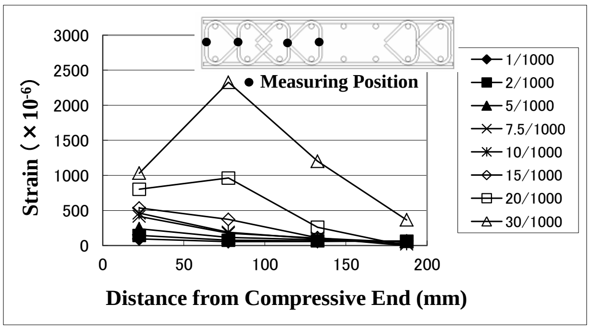

Fig. 6(b) Horizontal Strain Distribution of Confining bars (No.2)

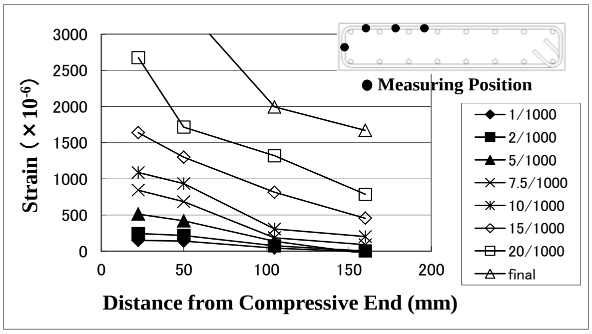

Fig. 6(c) Horizontal Strain Distribution of Hoop (No.7)

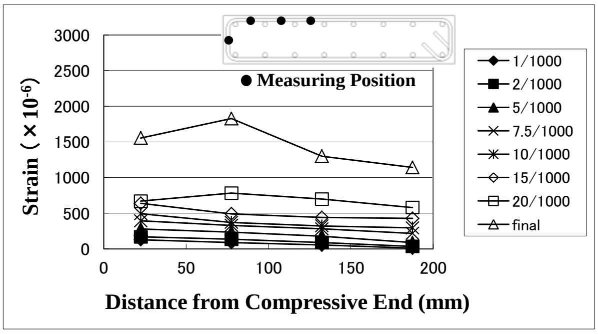

Fig. 6(d) Horizontal Strain Distribution of Hoop (No.8)

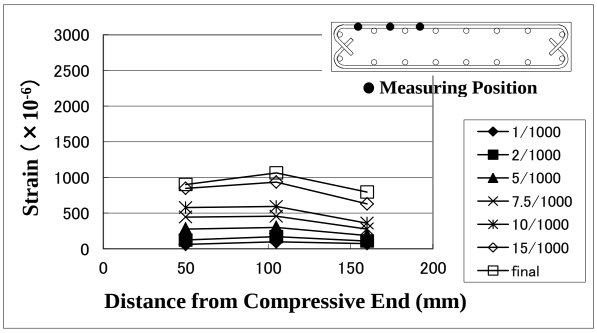

Fig. 6(e) Horizontal Strain Distribution of Transverse Reinforcement (H1)

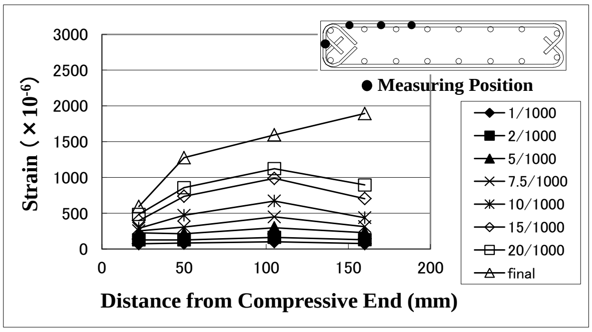

Fig. 6(f) Horizontal Strain Distribution of Confining bars and Transverse Reinforcement (H2)

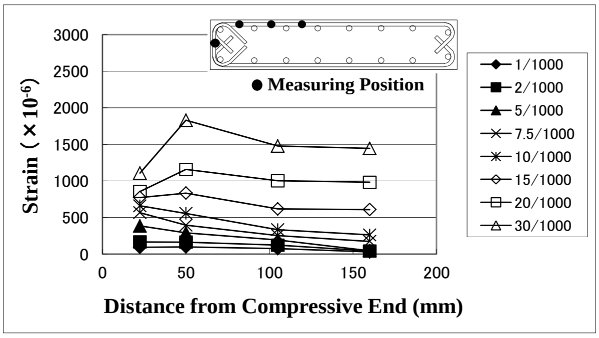

Fig. 6(g) Horizontal Strain Distribution of Confining bars and Transverse Reinforcement (H3)

in Specimen 8 was not remarkable and the strain in Specimen 8 was smaller than that in Specimen 7 as a whole. The reason for this tendency is considered to be that the neutral axis depth of Specimen 8 with an axial stress ratio of 0.4 was large and the high compressive area extended to the inside; therefore, the concrete confinement effect of the hoop became smaller.

In comparing Specimens H1 and H2 with the hook and an axial stress ratio of 0.4, the strain distribution in Specimen H1 without the confining bar was approximately the same as that of Specimen H2 with the confining bar until 20/1000. On the other hand, the strain in Specimen H2 increased largely at the final stage compared with that in Specimen H1. The reason for the increment is considered to be that the limit drift angle of Specimen H2 increased by the confinement effect of the confining bar in the thickness direction and therefore the strain of the transverse reinforcement increased. The increment of the strain of the transverse reinforcement was considered to show the confining force in the longitudinal direction in the cross section. It is considered that Specimen H1 had no confinement in the thickness direction, and therefore the concrete at the compressive end crumbled before the confining force was increased by the hook. The strain in Specimen H3 with the confining bar and an axial stress ratio of 0.2 was larger at the compressive area compared with Specimen H2 with the confining bar and an axial stress ratio of 0.4. The reason for this tendency is considered to be that the high compressive area in Specimen H3 was more concentrated at the edge area compared to Specimen H2 and the confining force increased.

4. CONCLUSIONS

Lateral loading tests were conducted on wall columns simulating the area near the corner of L-shaped core walls in order to examine the effect of edge confinement on the deformation capacity of core walls. Major findings are as follows:

(1) The larger drift angle ratio of a specimen corresponded to the larger number of confining bars and the smaller axial stress ratio.

(2) Specimens with four confining bars withstood the axial load up to 30/1000 at both axial stress ratios of 0.2 and 0.4 by arranging the confining bars further inside the cross section and confining the concrete in the area.

(3) In the case of specimens with the confining bar, the drift angle ratio of the specimens with the hook was larger than that without the hook.

(4) The specimens without the confining bars did not show the increment of the drift angle ratio by the hook. On the other hand, the drift angle ratio of the specimens with confining bars increased by the hook. It is considered that the specimen without the confining bars crumbled before the hook showed the concrete confinement effect.

REFERENCES

1) Nakachi, T., Toda, T., and Tabata, K. (1996). Experimental study of deformation capacity of reinforced concrete core walls after flexural yielding. *Proceedings of the 11th World Conference on Earthquake Engineering*, Paper No. 1714.
2) Hatakenaka, T., Nakachi, T. (2008). Study on deformation capacity of reinforced concrete core walls after flexural yielding. *Proceedings of the 14th World Conference on Earthquake Engineering*, Paper ID 12-01-0100.
3) Architectural Institute of Japan (AIJ). Ultimate strength and deformation capacity of buildings in seismic design. Gihodo Shuppan, Tokyo, 1990.